Programmed Death-1+ T Cells and Regulatory T Cells Are Enriched in Tumor-Involved Lymph Nodes and Associated with Aggressive Features in Papillary Thyroid Cancer

Jena D. French, Gregory R. Kotnis, Sherif Said, Christopher D. Raeburn, Robert C. McIntyre, Jr., Joshua P. Klopper, and Bryan R. Haugen

Department of Medicine (J.D.F., J.P.K., B.R.H.), Division of Endocrinology, Metabolism, and Diabetes, Departments of Pathology (S.S., B.R.H.) and Surgery (C.D.R., R.C.M.), and University of Colorado Cancer Center (J.D.F., J.P.K., B.R.H.), University of Colorado, Anschutz Medical Campus, Aurora, Colorado 80045; and Department of Anatomic Pathology (G.R.K.), Cleveland Clinic Foundation, Cleveland, Ohio 44195

Context: Recurrent metastatic lymph node (LN) disease is common in patients with papillary thyroid cancer (PTC). Novel prognostic markers may be helpful in guiding a therapeutic approach. Our previous studies revealed that immune suppression is evident in PTC and associated with more severe disease.

Objective: To characterize the immune response to metastatic PTC, we assessed CD4+ T cell polarization in LN. In addition, we investigated the role of programmed death-1 (PD-1) and T cell exhaustion.

Design: Uninvolved (UILN) and tumor-involved lymph nodes (TILN) were sampled *ex vivo* by fine-needle biopsy. T cell subsets were identified by flow cytometry. In parallel, archived TILN specimens were characterized by immunofluorescence.

Setting: The study was conducted at the University of Colorado Hospital.

Patients: Data were collected on 94 LN from 19 patients with PTC undergoing neck dissection.

Main Outcome: T cell subset frequencies were compared in UILN and TILN and assessed for correlation with recurrent disease and extranodal invasion.

Results: Regulatory CD4+ T cells (Treg) were enriched in TILN compared with UILN and further elevated in TILN from patients with recurrent disease. PD-1+ T cells were present at high frequency in TILN and markedly enriched in TILN that showed evidence of extranodal invasion. In TILN, Treg frequency correlated with PD-1+ T cell frequencies. Although PD-1+ T cells produced interferon-γ, they failed to fully down-regulate CD27 and were not actively proliferating.

Conclusions: Increased Treg and PD-1+ T cell frequencies in LN may be indicative of aggressive recurrent PTC. Future prospective studies are necessary to determine the prognostic and therapeutic value of these findings in PTC. (*J Clin Endocrinol Metab* 97: E934–E943, 2012)

The incidence of papillary thyroid cancer (PTC) is increasing (1). Despite the success of current therapies, 20–30% of PTC patients that have undergone primary thyroidectomy develop recurrence and/or metastases, most commonly in the locoregional lymph nodes (LN), requiring additional surgical intervention with increased morbidity and expense (2, 3). The extent of surgical LN dissection and use of adjuvant radioiodine therapy are still

Abbreviations: FNB, Fine-needle biopsy; Fox, Forkhead box; FVPTC, follicular variants of PTC; IFN, interferon; LN, lymph node; LT, lymphocytic thyroiditis; PD-1, programmed death-1; PTC, papillary thyroid cancer; Tg, thyroglobulin; TILN, tumor-involved lymph node; TPO, thyroperoxidase; Treg, regulatory CD4+ T cell; UILN, uninvolved tumor-involved lymph node.

highly debated in the management of patients with PTC. Identification of novel prognostic markers would be helpful in predicting the risk of disease recurrence and determining the extent of neck dissections or therapy needed to avoid persistent disease. Furthermore, patients with advance disease would benefit from novel adjuvant therapies. Our studies were designed to characterize the immune response in LN of patients with PTC, with the goal of identifying immune-relevant prognostic markers and targets for immune-based therapies.

Previous work by our laboratory revealed that tumor-associated lymphocytic infiltration is associated with more severe disease (4). Thus, despite the presence of a tumor-directed immune response, the host immune system is unsuccessful in eliminating the tumor and may even promote disease progression. In support of this theory, we found that increasing frequencies of $CD25^+$ Forkhead box (Fox) P3 regulatory $CD4^+$ T cells (Treg) correlated with a higher degree of LN metastasis in patients with PTC (4). Increased Treg frequencies in the peripheral blood, tumor, and lymph node have been associated with poor prognosis in other types of cancer (5–9). In addition to Treg, naive $CD4^+$ T cells can differentiate into at least three functionally distinct fates, Th1, Th2, or Th17, depending on the presence of key cytokines and the expression of specific transcription factors (10). Th1 polarization, which is characterized by the production of interferon (IFN)-γ and supports the cytotoxic $CD8^+$ T cell response, is known to promote tumor elimination (11). In contrast, a Th2 response, characterized by IL-4 production, is generally less protective and may encourage tumor progression (12). Both the antitumor and protumor properties of Th17 cells have been described, depending on the type of cancer and the stage of tumor development (13, 14). $CD4^+$ T cell polarization has not been assessed in patients with PTC.

T cell exhaustion is gaining support as an important mechanism of immune evasion in the tumor microenvironment (15). $CD4^+$ and $CD8^+$ T cell exhaustion were first characterized in models of chronic viral infections as a result of prolonged antigen exposure (16, 17). These cells display reduced proliferative potential and lose the ability to produce IL-2, TNFα, and IFNγ (17, 18). Exhausted T cells are characterized by sustained expression of inhibitory molecules, including programmed death-1 (PD-1), and a unique expression pattern of activation markers and cytokine receptors (19). For example, these cells fail to down-regulate CD27, which is normally reduced on activation. $PD-1^+$ T cells are enriched in tumors from patients with melanoma, renal cell carcinoma, lung cancer, prostate cancer, and ovarian cancer (20–24). The presence of $PD-1^+$ tumor-infiltrating T cells in renal cell carcinoma correlated with more severe disease (22). In melanoma, and ovarian cancer, tumor-associated $PD-1^+$ $CD8^+$ T cells were defective in their ability to produce IL-2 and IFNγ (20, 21).

To further define the T cell response in metastatic PTC, we sampled LN after surgical excision by fine-needle biopsy (FNB). We assessed both $CD4^+$ T cell polarization and signs of T cell exhaustion by flow cytometry and immunofluorescence. These studies are the first to characterize T cell phenotype in PTC and the first to investigate PD-1 and T cell exhaustion in metastatic LN.

Materials and Methods

Patients

Patients with PTC undergoing primary thyroidectomy and neck dissection or neck dissection for recurrent disease at University of Colorado Hospital between 2008 and 2010 were offered enrollment in this study. Patient sample analysis was performed following internal review board approval. LN from a total of 25 patients provided samples for this study. All patients with primary PTC were assessed for histological evidence of concurrent lymphocytic thyroiditis (LT). LT was assessed on a five-point semiquantitative scale: minimal (<10 lymphocytes), mild (50–100 lymphocytes), moderate (>100 lymphocytes), and severe (large confluent aggregates with frank germinal center formation). Patients scored as having moderate to severe LT were excluded from our analysis. Fifty-two percent of patients were tested for antithyroglobulin (Tg)/antithyroperoxidase (anti-TPO) levels. Seven of 14 patients categorized as minimal to mild were tested and only one patient (14%) was considered positive for anti-Tg. Six of 11 patients categorized as moderate to severe were tested, and three patients (50%) were considered positive for anti-Tg and/or anti-TPO.

The final PTC group included nine conventional PTC and five follicular variants of PTC (FVPTC). One conventional PTC patient (T1N0M0) displayed Hurthle cell features. The mean age was 44 ± 17 yr, and there were 10 females and four males in the group. Five tumor-involved lymph nodes (TILN) from one FVPTC patient with moderate $PD-1^+$ T cell frequency were excluded from T cell polarization analysis due to lack of corresponding Treg data. Five patients undergoing a secondary neck dissection for recurrent disease at least 1 yr after their primary surgery were also included in this study. All patients with recurrence were female with the average age of 43 ± 8 yr.

Standard American Joint Committee on Cancer (sixth edition) tumor node metastasis scoring was used for PTC staging (25). Pathology reports provided data on tumor type, tumor size, invasion, and LN metastases. Hematoxylin and eosin stains of LN sections were reevaluated to assess the presence, size, and invasiveness of tumor metastases. LN samples positive for extranodal invasion showed evidence of tumor penetration of the fibrous connective tissue capsule and the presence of metastatic tumor in extranodal soft tissue.

Fine-needle biopsies

LN were dissected from the submitted neck tissue by the pathologist (G.R.K. or S.S.). Lymphocytes were obtained from LN by FNB using a 25-gauge needle and 5-ml syringe. The needle

was inserted into the tissue and pulsated in multiple directions to obtain a representative sample. Three milliliters of culture media were added to the open syringe, and the plunger was used to push the media and cells into a collection tube. Up to 8 LN were sampled from each patient. LN were inked with distinct colors and logged, allowing for later histological analysis. Each node was defined as uninvolved or involved and the size and invasive characteristics of metastases were noted. The number of samples generated was limited by the ability to detect LN in the specimen by gross analysis, the size of the LN, and the amount of lymphoid tissue remaining in the node. Biopsy specimens were cultured overnight at 37 C in RPMI 1640 containing L-glutamine, 5% fetal bovine serum, 20 U/ml penicillin, and 20 μl/ml streptomycin. Because cell number was limiting in these fresh biopsies, we were unable to count or assess viability. Those samples that showed visual evidence of poor lymphocyte yield or viability were omitted from further analysis.

Flow cytometry

Lymphocytes obtained from LN biopsies were activated for 4 h with 50 ng/ml phorbol 12-myristate 13-acetate (Sigma, St. Louis, MO) and 0.5 μg/ml ionomycin (Sigma) in the presence of GolgiPlug (1:500; BD Biosciences, Franklin Lakes, NJ) and harvested in PBS/1% fetal bovine serum/0.1% sodium azide for staining. Cells were preincubated with FcRγ block (eBioscience, San Diego, CA); stained with antibodies specific for CD3, CD4, and CD8; washed; and split for subsequent staining. Samples were stained for CD25 or PD-1, CD27, and CD45RA, washed, resuspended in 1$\times$ fixation/permeabilization buffer (eBioscience), and incubated overnight at 4 C. Cells were transferred into 1$\times$ permeabilization buffer (eBioscience) and stained for intracellular FoxP3, cytotoxic T lymphocyte-associated antigen 4, IL-4, and IL-17 or IFNγ. Cells were fixed with 1% paraformaldehyde and analyzed with the Gallios flow cytometer (Beckman Coulter, Fullerton, CA). Single-color controls were generated with matched fluorochrome-conjugated antibodies and CompBeads (BD Biosciences). Data were processed using Flowjo software (Tree Star, Inc., Ashland, OR). Viable lymphocytes were gated according to light scatter. On average, we collected 4.3 $\times$ 10^4 live lymphocyte events and 2.6 $\times$ 10^4 CD3$^+$ events. Due the heterogeneity of these fresh, unsorted samples, the number of T cells analyzed was variable. Gating strategies were determined using peripheral blood lymphocytes. Subset frequencies were determined as the percentage of CD4$^+$ or CD8$^+$ T cells. Researchers were blinded to clinical characteristics and LN involvement during data analysis.

Immunofluorescence

LN specimens were formalin fixed and paraffin embedded after FNB and 4-μm tissue sections were prepared. Tissue sections were deparaffinized and rehydrated in ethanol using standard protocols. Antigen retrieval was performed in 10 mM citrate buffer (pH 6; 5 min, 120 C) in the decloaking chamber (Biocare Medical, Concord, CA). Tissues were blocked with 5% normal goat serum plus 1% BSA in PBS for 1 h at room temperature and stained with primary antibodies overnight at 4C (anti-PD-1, 1:50; Abcam, Cambridge, MA; anti-Ki67, 1:100; Invitrogen, Carlsbad, CA). Staining was detected with goat antibodies against mouse IgG1-AF647 and rabbit IgG-AF546 (PD-1/Ki67; Invitrogen). Tissues were counterstained with 4′,6′-diamino-2-phenylindole for 20 min at room temperature and mounted with Fluoromount-G (SouthernBiotech, Birmingham, AL). Fluorescent images were obtained at $\times$10 and $\times$60 using the Spinning Disk IX81 microscope (Olympus, Tokyo. Japan) and Slidebook software (3i, Inc., Denver, CO). Ki67$^+$/PD-1$^+$ lymphocytes were quantified using ImageJ software (National Institutes of Health, Bethesda, MD). For each TILN, a minimum of eight representative images was captured in areas in which PD-1$^+$ T cells were evident. Total PD-1$^+$ and Ki-67$^+$PD-1$^+$ counts were combined from all fields, and the percentage of Ki67$^+$PD-1$^+$ cells of total PD-1$^+$ lymphocytes was calculated. PD-1$^+$ lymphocyte counts ranged from 109 to 652.

Antibodies

Anti-CD3-alexafluor-700 (UCHT1), anti-CD4-fitc (RPA-T4), anti-FoxP3-PE (PCH101), anti-IL-4-PE-Cy7 (8D4-8), and anti-IL-17A-alexafluor-647 (eBio64DEC17), anti-IFNγ-PerCP-Cy5.5 (4S.B3), anti-CD45RA-PE (HI100), anti-CD27-PE-Cy7 (LG.7F9), and anti-CLTA-4-biotin (14D3) were purchased from eBioscience. Anti-PD-1-AF647 (EH12.1) and anti-CD25-APC-Cy7 (M-A251) were purchased from BD PharMingen (San Diego, CA). Anti-CD8-Pacific Orange (MHCDO830) was purchased from Invitrogen.

Statistical analysis

To determine the statistical significance of interval data, we used the Mann Whitney nonparametric *t* test. Correlations between lymphocyte subset frequencies were determined by calculating the Spearman correlation coefficient. The level of statistical significance, with 95% confidence, was adjusted using the Bonferroni correction for each analysis.

Results

Treg are enriched in TILN and further increased in patients with recurrent disease

To investigate the immune response in patients with metastatic PTC, we biopsied LN from patients with PTC undergoing primary thyroidectomy and neck dissection for suspected LN involvement. Eleven of the 25 patients

TABLE 1. Clinical summary of LN biopsy patients

	Number of patients	Number of LN analyzed	
		UILN	TILN
PTC with LT	11	63	5
PTC without LT	14	38	28
PTC	9	23	24
FVPTC	5	15	4
pN0	6	16	n/a
pN1	8	22	28
Central neck (N1a)		12	21
Lateral neck (N1b)		10	7
Stage I	9	24	20
Stage II	0	0	0
Stage III	4	5	5
Stage IV	1	9	3
PTC with recurrent LN disease	5	13	15

sampled were determined to have LT. Of the 342 LN removed from patients with LT, only 12 contained metastatic tumor (3.5%, data not shown). As shown in Table 1, we obtained biopsy samples from 63 uninvolved tumor-involved LN (UILN) and only five TILN. This discrepancy in sample size precluded analysis of TILN in LT patients.

Furthermore, previous data from our group suggest that the immune response in patients with LT is distinct from the antitumor response in PTC patients (4). To characterize the tumor-directed immune response, we sampled UILN and TILN from patients who showed no histological evidence of LT. Biopsies were obtained from 14 PTC
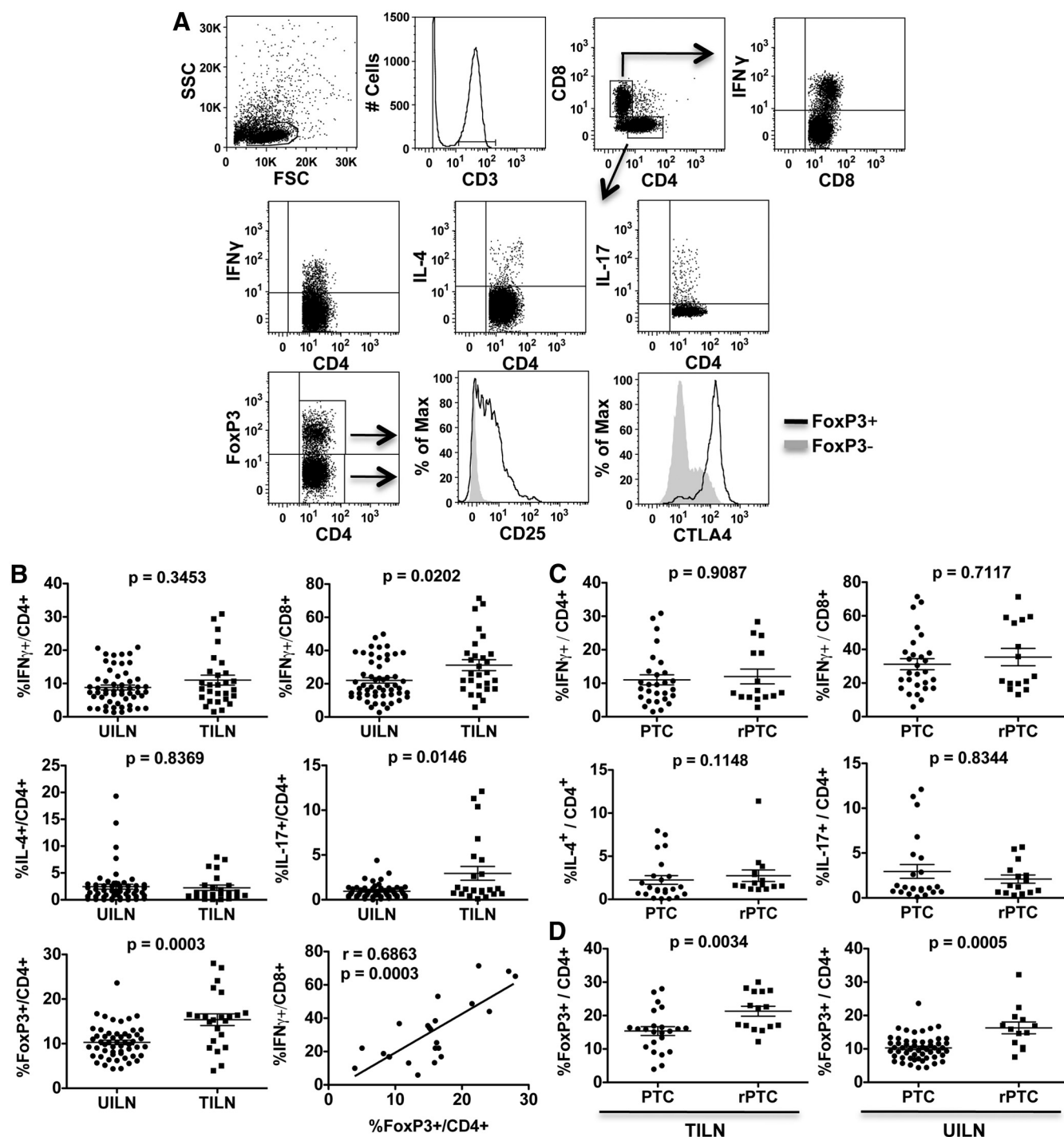
FIG. 1. Analysis of T lymphocyte polarization in UILN and TILN by flow cytometry. Biopsies were obtained from UILN and TILN, and T cell subsets were analyzed by flow cytometry. A, A representative sample and the gating strategy is shown. B, CD4$^+$ and CD8$^+$ T cell subset frequencies were compared in UILN and TILN from patients with primary PTC. C, T cell subset frequencies were compared in TILN from patients with primary disease (PTC) and recurrent PTC (rPTC). D, Treg frequencies were compared in primary and recurrent patients in both TILN and UILN. Mean ± SEM is shown. Values of $P < 0.01$ were considered significant.

patients, eight of whom had metastatic disease (pN1, Table 1). In total, 330 LN were removed from these patients, and 73 of these were determined to contain metastatic PTC (22.1%, data not shown). Of these potential specimens, 94 LN were sampled and 38 UILN and 28 TILN LN generated adequate samples for our analysis.

Lymphocytes recovered from LN were activated *in vitro* and analyzed by flow cytometry. As shown in Fig. 1A, $CD4^+$ T cells were assessed for their expression of $IFN\gamma$ (Th1), IL-4 (Th2), IL-17 (Th17), and FoxP3 (Treg). $FoxP3^+ CD4^+$ Treg consistently expressed CD25 and cytotoxic T lymphocyte-associated antigen 4 (Fig. 1A). $CD8^+$ T cells were assessed for intracellular expression of $IFN\gamma$ (Fig. 1A). On average, $IFN\gamma^+CD8^+$, but not $IFN\gamma^+CD4^+$, T cells were enriched in TILN compared with UILN (Fig. 1B). Th2 cell frequency was not significantly different in UILN and TILN (Fig. 1B). Th17 cells were found at low levels in the majority of UILN and

TILN; however, a small subset of TILN showed evidence of Th17 polarization (>5% of $CD4^+$ T cells, Fig. 1B). $CD4^+FoxP3^+$ Treg showed the most significant increase in TILN, constituting 14% of the $CD4^+$ T cell population on average when tumor metastases were present compared with 10% in UILN (Fig. 1B), although there was overlap between the groups. Despite the presence of Treg, in many LN, a significant portion of $CD4^+$ and $CD8^+$ T cells produced $IFN\gamma$. Of interest, Treg frequency correlated directly with the frequency of $IFN\gamma^+ CD8^+$ (Fig. 1B) and $CD4^+$ (r = 0.7532, P < 0.0001; data not shown) T cells in TILN. No statistically significant association was found in UILN (data not shown).

To assess Th polarization in patients with recurrent disease, we collected biopsies from patients undergoing neck dissection at least 1 yr after their original thyroidectomy. As shown in Fig. 1C, no significant change was observed in the average frequency of $IFN\gamma^+CD4^+$, $IFN\gamma^+CD8^+$, Th2, or Th17 subsets in TILN from patients with recurrent disease compared with those with primary PTC. In contrast, Treg were more abundant in TILN from recurrent PTC patients compared with TILN from primary surgeries (Fig. 1D). Of note, the frequency of Treg was also increased on average in UILN from patients with recurrent compared with primary disease (Fig. 1D). As in patients with primary disease, Treg levels were significantly elevated in TILN compared with UILN in patients with recurrent disease (Fig. 1D; recurrent PTC, *left panel vs. right panel*; P = 0.032).

$PD-1^+$ T cells are enriched in TILN and their frequency correlates with Treg

To further investigate the functional capacity of T cells in patients with metastatic PTC, we assessed expression of PD-1, which is transiently induced during T cell activation (26) and expressed constitutively by exhausted, dysfunctional T cells (19). UILN and TILN biopsies were stained for T cell-specific markers and PD-1 and analyzed by flow cytometry. As shown in Fig. 2A, $PD-1^+CD4^+$ and $PD-1^+CD8^+$ T cell frequencies were increased on average in TILN compared with UILN. In 8 of 28 and 11 of 28 TILN, $PD-1^+$ cells constituted greater than 40% of the $CD4^+$ and $CD8^+$ T cell populations, respec-
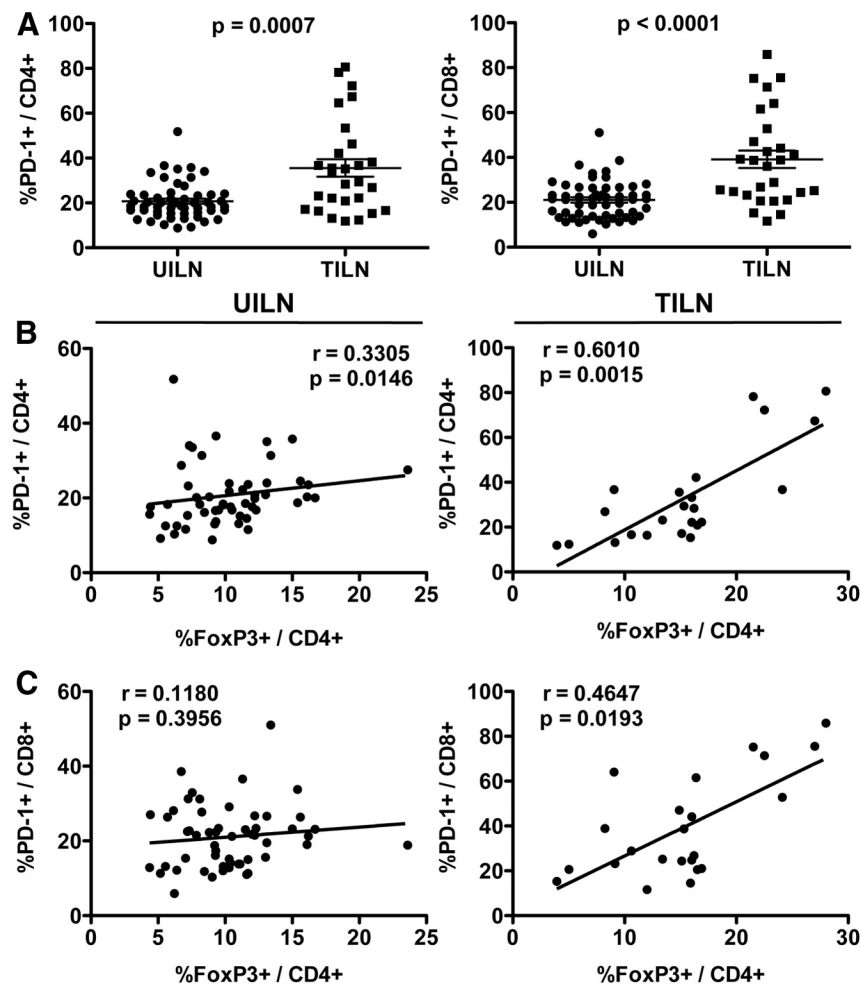

FIG. 2. $PD-1^+$ T cell frequency in UILN and TILN. A, Biopsies were obtained from UILN and TILN, and $PD-1^+$ T cell frequency was determined by flow cytometry. Cumulative graphs showing the percentage of $PD-1^+$ cells in the general $CD4^+$ and $CD8^+$ T cell populations in UILN and TILN. Mean ± SEM is shown. $FoxP3^+/CD4^+$ Treg and $PD-1^+/CD4^+$ (B) or $PD-1^+/CD8^+$ (C) T cells frequencies were compared in UILN and TILN. Values of P < 0.025 were considered significant.

tively, reaching as high as 80% in some samples. PD-1$^+$ T cells and Treg are known to coinfiltrate breast carcinomas (27). We next investigated whether increased PD-1$^+$ T cell frequency was associated with high levels of Treg in metastatic PTC. PD-1$^+$CD4$^+$ T cells correlated weakly with Treg in UILN but showed a strong and statistically significant correlation in TILN (Fig. 2B). As shown in Fig. 2C, PD-1$^+$CD8$^+$ T cell and Treg frequencies correlated in TILN but not in UILN. Of note, Treg have been shown to express PD-1 (28). To determine whether Treg accounted

for a significant portion of PD-1$^+$CD4$^+$ T cells, we analyzed archived TILN sections by immunofluorescence for PD-1 and FoxP3. Although PD-1$^+$ Treg were present in TILN, the majority of Treg lacked PD-1 expression (data not shown).

PD-1$^+$ T cells in TILN show signs of activation and exhaustion

To determine whether PD-1 is expressed as a marker of early activation or T cell exhaustion, we assessed
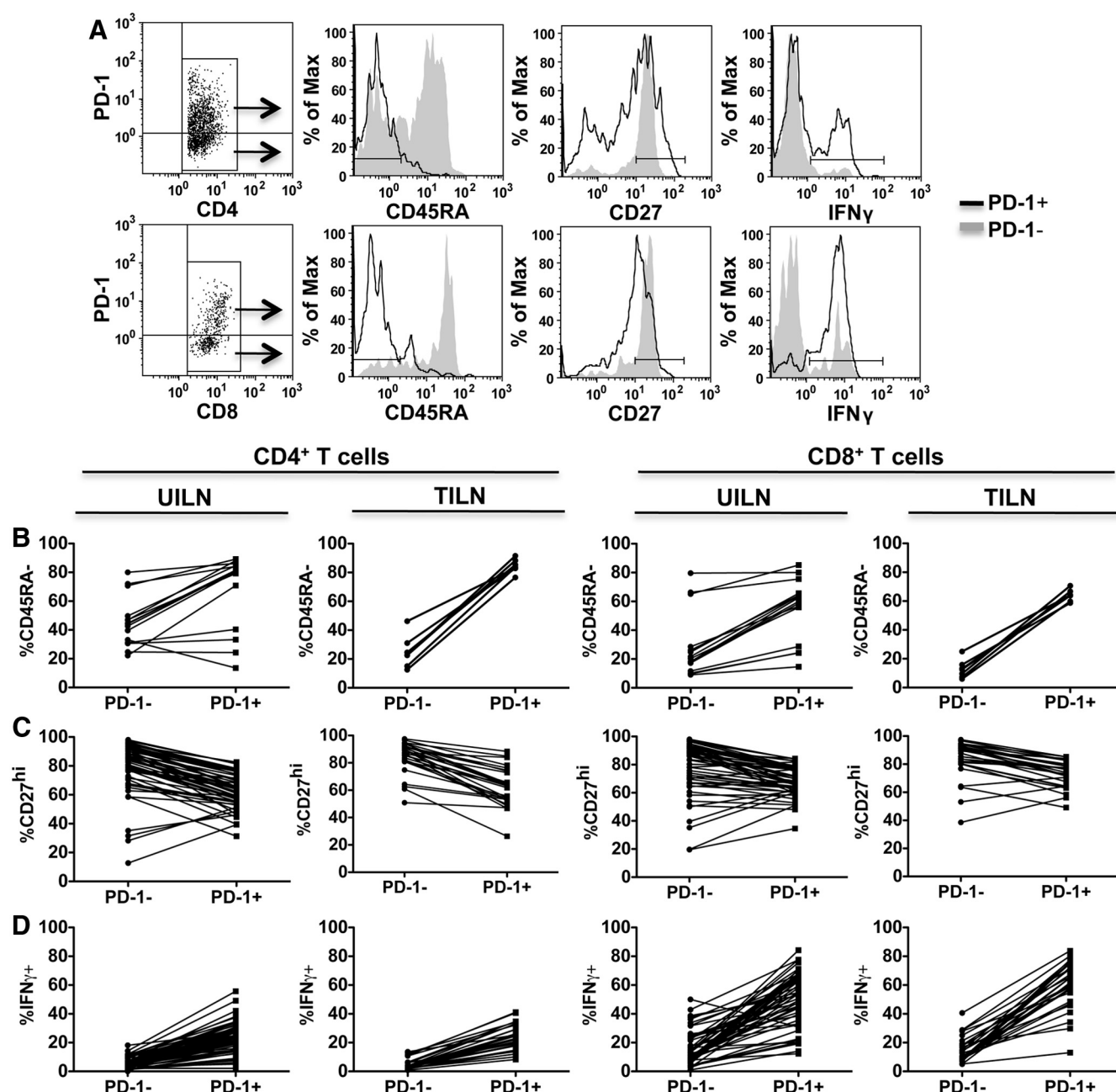
FIG. 3. PD-1$^+$ T cell phenotype in UILN and TILN. A, Flow cytometry analysis of PD-1$^+$ and PD-1$^-$ CD4$^+$ (*top row*) or CD8$^+$ (*bottom row*) T cells. A representative TILN biopsy is shown. Matched PD-1$^-$ and PD-1$^+$ CD4 or CD8 T cells from each UILN or TILN were compared for expression of CD45RA (B) CD27 (C), and IFNγ (D). A subset of the patients contributed data for CD45RA (UILN, n = 9; TILN, n = 7) and CD27 (UILN, n = 37; TILN, n = 27).

expression of CD45RA, CD27, and intracellular IFNγ by PD-1⁻ and PD-1⁺ T cells by flow cytometry (Fig. 3). PD-1⁻ T cells, presumed to represent naïve or resting memory T cells (29), were compared with the corresponding PD-1⁺ T cell populations in each UILN and TILN. PD-1⁺ T cell in TILN were largely CD45RA⁻ memory cells, whereas the majority of PD-1⁻ T cells were CD45RA⁺ (Fig. 3, A and B). In contrast, in UILN the frequency of CD45RA⁻ memory cells was variable in both PD1⁻ and PD-1⁺ T cell subsets (Fig. 3B). CD27 is expressed at high levels on resting T cells, is down-regulated after activation, and remains high on exhausted PD-1⁺ T cells (19). In a large portion of UILN and TILN, the frequency of CD27ʰⁱ T cells was reduced in the PD-1⁺ population compared with PD-1⁻ cells, suggesting that a portion of PD-1⁺ T cells had begun to down-regulate CD27. However, greater than 50% of PD-1⁺CD4⁺ and PD-1⁺CD8⁺ T cells maintained a high expression of CD27 in 22 of 27 and 26 of 27 of TILN and 45 of 53 and 51 of 53 UILN, respectively (Fig. 3, A and C). To determine whether, PD-1⁺ T cells were capable of producing effector cytokines, we assessed IFNγ production after nonspecific stimulation *in vitro*. IFNγ-producing PD-1⁺ CD4⁺, and CD8⁺ T cells were found at similar or increased frequencies compared with PD-1⁻ T cells in both TILN and UILN (Fig. 3D). Exhausted T cells are compromised in their ability to pro-

liferate (19, 30). To assess the proliferative status of PD-1⁺ T cells in TILN, we stained archived LN sections for PD-1 and Ki67 using standard immunofluoresence techniques (Fig. 4). Although PD-1 and Ki67 staining was sparse in some samples (Fig. 4A), other TILN contained dense populations of PD-1⁺ and Ki67⁺ lymphocytes (Fig. 4B). Of note, Ki67⁺PD-1⁺ lymphocytes were rare in these samples, such that less than 20% of PD-1⁺ cells showed signs of proliferation in the 12 TILN assessed (5.7–18.8%, Fig. 4, C and D).

Higher PD-1⁺ T cell frequency is associated with extranodal invasion

Extranodal invasion has been linked to disease recurrence in PTC (31). To investigate the role of Treg and PD-1⁺ T cells in extranodal invasion, TILN were assessed for evidence of capsule penetration and the presence of metastatic tumor in extranodal soft tissue and grouped accordingly. Although a subset of TILN with extranodal invasion had the highest frequency of Treg, a statistically significant difference in Treg levels was not observed between noninvasive and invasive metastases (Fig. 5A). Both PD-1⁺CD4⁺ (Fig. 5B) and PD-1⁺CD8⁺ (Fig. 5C) T cell frequencies were significantly higher on average in TILN with extranodal invasion compared with those with noninvasive LN metastases.
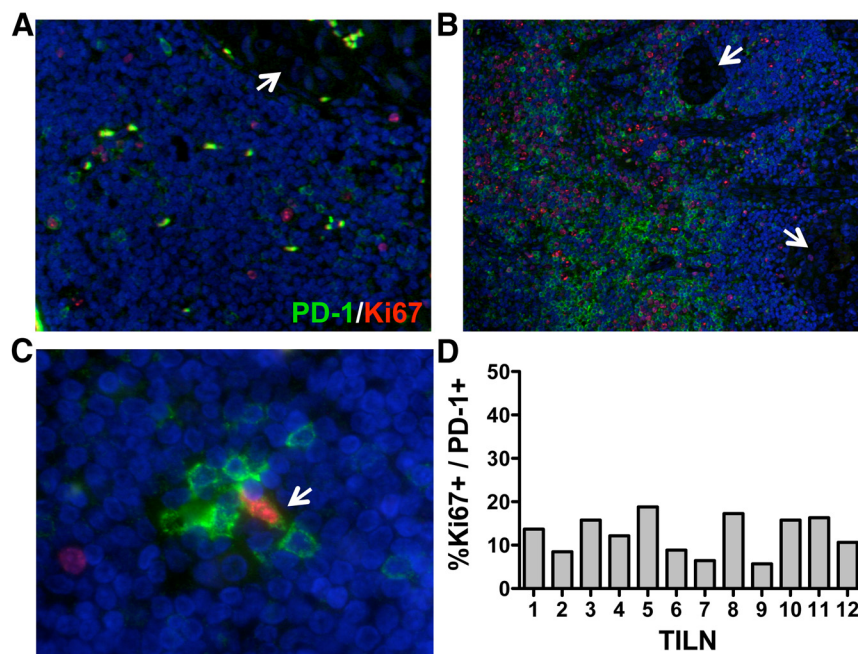

FIG. 4. Immunofluorescence analysis of PD-1 and Ki-67 in TILN. Lymph node tissue sections were stained for PD-1 (*green*) and Ki-67 (*red*) (A–C). Images were obtained at ×10 (A, LN4; and B, LN8) or ×60 (C, LN6) magnification. *White arrows* designated PTC metastasis (A and B). C, A single PD-1⁺Ki67⁺ lymphocyte is identified (*white arrow*) among PD-1⁺Ki67⁻ lymphocytes. D, The frequency of PD-1⁺Ki67⁺ lymphocytes in the total PD-1⁺ population is shown for 12 TILN obtained from two patients with metastatic disease.

Discussion

Our previous studies in primary PTC nodules suggest that immune suppression contributes to disease progression (4). Here we analyzed the immune response in LN from patients with PTC. Th1 polarization and high levels of IFNγ⁺CD8⁺ T cells were evident in many LN from patients with primary and recurrent PTC. Thus, the presence of metastases does not deter, and may even promote, an IFNγ response. Th1-polarization in many LN suggests that a productive antitumor response had been generated. In support of this hypothesis, proliferating lymphocytes were evident in TILN, including those in which only minimal LN tissue remained intact. These data may explain, in part, why LN metastasis is not a strong predictor of survival or disease progression in PTC.

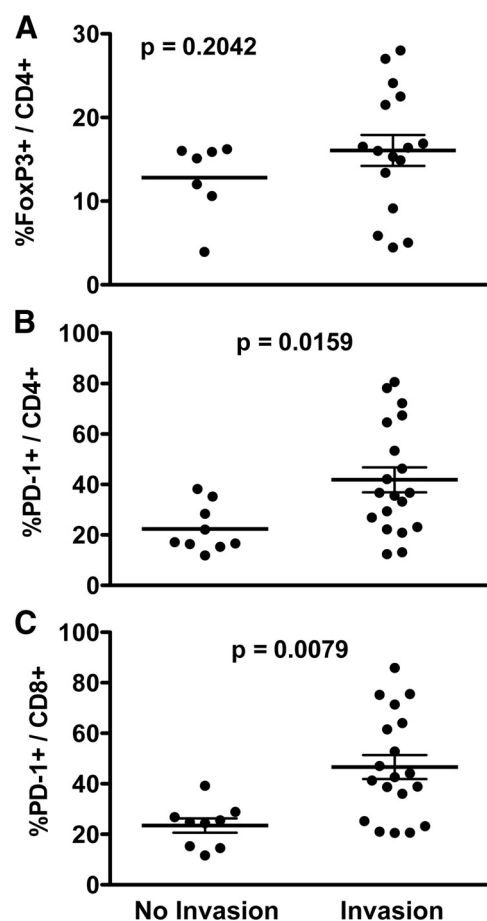At the same time, however, Treg were elevated in the presence of meta-

FIG. 5. PD-1$^+$ T cells, Treg, and extranodal invasion. PD-1$^+$ T cell and Treg frequencies in each UILN and TILN were determined by flow cytometry. Archived TILN samples were analyzed for evidence of extranodal invasion by hematoxylin and eosin stain. Samples were grouped according to the absence or presence of invasion, and the frequency of FoxP3$^+$CD4$^+$ Treg (A), PD-1$^+$CD4$^+$ (B), or PD-1$^+$CD8$^+$ (C) T cells in each lymph node is shown. Mean ± SEM is shown. Values of P < 0.017 were considered significant.

static disease and an increased frequency of Treg was associated with a prominent IFNγ response. Although Treg may be induced in these LN as a compensatory mechanism to maintain immune homeostasis, our observed association between elevated Treg levels and recurrent disease supports that hypothesis that Treg are induced by the resident metastatic tumor in an attempt to evade the immune response. Of interest, Treg were elevated in UILN from patients with recurrent disease compared with those from primary PTC patients. Thus, despite the absence of resident tumor, UILN in these patients may be subjected to suppressive effects in nearby TILN (32), priming the node for future metastases.

To begin to address the functional capacity of the T cell response in patients with PTC, we investigated whether these cells expressed PD-1. We discovered that PD-1$^+$ T cells constitute a significant portion of both CD4$^+$ and CD8$^+$ T cell populations in TILN. PD-1$^+$ T cells in TILN

were primarily CD45RA$^-$, suggesting that they had recently encountered their requisite antigen. However, these cells were largely negative for Ki-67 staining. Thus, unlike classic memory T cells that down-regulate CD45RA and proliferate after antigen stimulation (33), PTC-associated PD-1$^+$ T cells show little sign of active or recent proliferation. Furthermore, a subset of PD-1$^+$ T cells failed to fully down-regulate CD27. In the chronic lymphocytic choriomeningitis virus model of T cell exhaustion, CD27 expression remains high on virus-specific exhausted T cells. In contrast, virus-specific T cells reduce CD27 to intermediate and low expression levels during acute infection in which exhaustion is not observed (19). In our studies, PD-1$^+$ T cells expressing intermediate or low levels of CD27 may represent acute activation in response to tumor or nontumor antigens, whereas CD27^{hi}PD-1$^+$ T cells may be dysfunctional and may be progressing toward exhaustion. Although additional studies are necessary to determine the functional competence of PD-1$^+$ T cells in metastatic PTC, high frequencies of PD-1$^+$ T cells in TILN with invasive tumors are likely a sign of immune suppression in the presence of aggressive metastases.

Of interest, PD-1$^+$ T cells maintained the ability to produce IFNγ after nonspecific stimulation *in vitro*. This finding contrasts that seen in melanoma-associated PD-1$^+$CD8$^+$ T cells in which IFNγ production was diminished in five of six patients (20). However, transient effector function has been observed in T cells during the process of peripheral tolerance (34, 35). Thus, our findings could represent intermediate stages of T cell activation during the establishment of T cell tolerance to thyroid cancer. These data must be interpreted cautiously because *in vitro* stimulation with phorbol 12-myristate 13-acetate and ionomycin bypass early signal transduction pathways downstream of T cell receptor (36). Although an accurate picture of polarization can be obtained, the functional integrity of tumor-associated T cells cannot be assessed in the absence of a more physiologically relevant stimulus. Although a number of potential tumor antigens exist in PTC, tumor-specific T cell epitopes have not been defined. This information will be essential to accurately characterize the role of T cell exhaustion in PTC.

In summary, our studies reveal that high frequencies of PD-1$^+$ T cells and Treg in TILN are associated with extranodal invasion and recurrence, respectively. These analyses used *ex vivo* FNB techniques that could be readily adapted as a presurgical *in vivo* screen of suspicious LN. Larger prospective studies are necessary to determine the potential of PD-1$^+$ T cell and Treg frequencies as prognostic factors in metastatic PTC. A recent clinical trial assessing the efficacy of the PD-1-blocking antibody, MDX-1106, in cancer therapy showed promising results

with minimal adverse effects (37). A more detailed analysis of PTC-specific PD-1$^+$ T cells may encourage the use of MDX-1106 for recurrent or advanced PTC that cannot be cured with surgery or standard therapies.

Acknowledgments

References

1. **Davies L, Welch HG** 2006 Increasing incidence of thyroid cancer in the United States, 1973–2002. JAMA 295:2164–2167
2. **Mazzaferri EL, Jhiang SM** 1994 Long-term impact of initial surgical and medical therapy on papillary and follicular thyroid cancer. Am J Med 97:418–428
3. **National Cancer Institute** 2007 Surveillance Epidemiology and End Results (SEER): cancer statistics review, 1973–2005. National Institutes of Health: www.cancer.gov
4. **French JD, Weber ZJ, Fretwell DL, Said S, Klopper JP, Haugen BR** 2010 Tumor-associated lymphocytes and increased FoxP3+ regulatory T cell frequency correlate with more aggressive papillary thyroid cancer. J Clin Endocrinol Metab 95:2325–2333
5. **Bates GJ, Fox SB, Han C, Leek RD, Garcia JF, Harris AL, Banham AH** 2006 Quantification of regulatory T cells enables the identification of high-risk breast cancer patients and those at risk of late relapse. J Clin Oncol 24:5373–5380
6. **Carreras J, Lopez-Guillermo A, Fox BC, Colomo L, Martinez A, Roncador G, Montserrat E, Campo E, Banham AH** 2006 High numbers of tumor-infiltrating FOXP3-positive regulatory T cells are associated with improved overall survival in follicular lymphoma. Blood 108:2957–2964
7. **Deng L, Zhang H, Luan Y, Zhang J, Xing Q, Dong S, Wu X, Liu M, Wang S** 2010 Accumulation of foxp3+ T regulatory cells in draining lymph nodes correlates with disease progression and immune suppression in colorectal cancer patients. Clin Cancer Res 16:4105–4112
8. **Nakamura R, Sakakibara M, Nagashima T, Sangai T, Arai M, Fujimori T, Takano S, Shida T, Nakatani Y, Miyazaki M** 2009 Accumulation of regulatory T cells in sentinel lymph nodes is a prognostic predictor in patients with node-negative breast cancer. Eur J Cancer 45:2123–2131
9. **Wolf D, Wolf AM, Rumpold H, Fiegl H, Zeimet AG, Muller-Holzner E, Deibl M, Gastl G, Gunsilius E, Marth C** 2005 The expression of the regulatory T cell-specific forkhead box transcription factor FoxP3 is associated with poor prognosis in ovarian cancer. Clin Cancer Res 11:8326–8331
10. **Zhu J, Paul WE** 2008 CD4 T cells: fates, functions, and faults. Blood 112:1557–1569
11. **Dighe AS, Richards E, Old LJ, Schreiber RD** 1994 Enhanced in vivo growth and resistance to rejection of tumor cells expressing dominant negative IFN γ receptors. Immunity 1:447–456
12. **Tan TT, Coussens LM** 2007 Humoral immunity, inflammation and cancer. Curr Opin Immunol 19:209–216
13. **Murugaiyan G, Saha B** 2009 Protumor vs antitumor functions of IL-17. J Immunol 183:4169–4175
14. **Numasaki M, Fukushi J, Ono M, Narula SK, Zavodny PJ, Kudo T, Robbins PD, Tahara H, Lotze MT** 2003 Interleukin-17 promotes angiogenesis and tumor growth. Blood 101:2620–2627
15. **Kim PS, Ahmed R** 2010 Features of responding T cells in cancer and chronic infection. Curr Opin Immunol 22:223–230
16. **Brooks DG, Teyton L, Oldstone MB, McGavern DB** 2005 Intrinsic functional dysregulation of CD4 T cells occurs rapidly following persistent viral infection. J Virol 79:10514–10527
17. **Wherry EJ, Blattman JN, Murali-Krishna K, van der Most R, Ahmed R** 2003 Viral persistence alters CD8 T-cell immunodominance and tissue distribution and results in distinct stages of functional impairment. J Virol 77:4911–4927
18. **Barber DL, Wherry EJ, Masopust D, Zhu B, Allison JP, Sharpe AH, Freeman GJ, Ahmed R** 2006 Restoring function in exhausted CD8 T cells during chronic viral infection. Nature 439:682–687
19. **Wherry EJ, Ha SJ, Kaech SM, Haining WN, Sarkar S, Kalia V, Subramaniam S, Blattman JN, Barber DL, Ahmed R** 2007 Molecular signature of CD8+ T cell exhaustion during chronic viral infection. Immunity 27:670–684
20. **Ahmadzadeh M, Johnson LA, Heemskerk B, Wunderlich JR, Dudley ME, White DE, Rosenberg SA** 2009 Tumor antigen-specific CD8 T cells infiltrating the tumor express high levels of PD-1 and are functionally impaired. Blood 114:1537–1544
21. **Matsuzaki J, Gnjatic S, Mhawech-Fauceglia P, Beck A, Miller A, Tsuji T, Eppolito C, Qian F, Lele S, Shrikant P, Old LJ, Odunsi K** 2010 Tumor-infiltrating NY-ESO-1-specific CD8+ T cells are negatively regulated by LAG-3 and PD-1 in human ovarian cancer. Proc Natl Acad Sci USA 107:7875–7880
22. **Thompson RH, Dong H, Lohse CM, Leibovich BC, Blute ML, Cheville JC, Kwon ED** 2007 PD-1 is expressed by tumor-infiltrating immune cells and is associated with poor outcome for patients with renal cell carcinoma. Clin Cancer Res 13:1757–1761
23. **Sfanos KS, Bruno TC, Meeker AK, De Marzo AM, Isaacs WB, Drake CG** 2009 Human prostate-infiltrating CD8+ T lymphocytes are oligoclonal and PD-1+. Prostate 69:1694–1703
24. **Zhang Y, Huang S, Gong D, Qin Y, Shen Q** 2010 Programmed death-1 upregulation is correlated with dysfunction of tumor-infiltrating CD8+ T lymphocytes in human non-small cell lung cancer. Cell Mol Immunol 7:389–395
25. **American Joint Committee on Cancer** 2002 AJCC cancer staging handbook: TNM classification of malignant tumors, 6th ed. New York: Springer
26. **Vibhakar R, Juan G, Traganos F, Darzynkiewicz Z, Finger LR** 1997 Activation-induced expression of human programmed death-1 gene in T-lymphocytes. Exp Cell Res 232:25–28
27. **Ghebeh H, Barhoush E, Tulbah A, Elkum N, Al-Tweigeri T, Dermime S** 2008 FOXP3+ Tregs and B7-H1+/PD-1+ T lymphocytes

co-infiltrate the tumor tissues of high-risk breast cancer patients: Implication for immunotherapy. BMC Cancer 8:57–68

28. **Kryczek I, Liu R, Wang G, Wu K, Shu X, Szeliga W, Vatan L, Finlayson E, Huang E, Simeone D, Redman B, Welling TH, Chang A, Zou W** 2009 FOXP3 defines regulatory T cells in human tumor and autoimmune disease. Cancer Res 69:3995–4000

29. **Agata Y, Kawasaki A, Nishimura H, Ishida Y, Tsubata T, Yagita H, Honjo T** 1996 Expression of the PD-1 antigen on the surface of stimulated mouse T and B lymphocytes. Int Immunol 8:765–772

30. **Wherry EJ, Barber DL, Kaech SM, Blattman JN, Ahmed R** 2004 Antigen-independent memory CD8 T cells do not develop during chronic viral infection. Proc Natl Acad Sci USA 101:16004–16009

31. **Ito Y, Fukushima M, Tomoda C, Inoue H, Kihara M, Higashiyama T, Uruno T, Takamura Y, Miya A, Kobayashi K, Matsuzuka F, Miyauchi A** 2009 Prognosis of patients with papillary thyroid carcinoma having clinically apparent metastasis to the lateral compartment. Endocr J 56:759–766

32. **Wen DR, Hoon DS, Chang C, Cochran AJ** 1989 Variations in lymphokine generation by individual lymph nodes draining human malignant tumors. Cancer Immunol Immunother 30:277–282

33. **Carrasco J, Godelaine D, Van Pel A, Boon T, van der Bruggen P**

34. **DuPage M, Cheung AF, Mazumdar C, Winslow MM, Bronson R, Schmidt LM, Crowley D, Chen J, Jacks T** 2011 Endogenous T cell responses to antigens expressed in lung adenocarcinomas delay malignant tumor progression. Cancer Cell 19:72–85

35. **Huang X, Yang Y** 2004 Transient gain of effector function by CD8+ T cells undergoing peripheral tolerance to high-dose self-antigen. Eur J Immunol 34:1351–1360

36. **Wang SF, Fouquet S, Chapon M, Salmon H, Regnier F, Labroquère K, Badoual C, Damotte D, Validire P, Maubec E, Delongchamps NB, Cazes A, Gibault L, Garcette M, Dieu-Nosjean MC, Zerbib M, Avril MF, Prévost-Blondel A, Randriamampita C, Trautmann A, Bercovici N** 2011 Early T cell signalling is reversibly altered in PD-1 T lymphocytes infiltrating human tumors. PLoS One 6:e17621

37. **Brahmer JR, Drake CG, Wollner I, Powderly JD, Picus J, Sharfman WH, Stankevich E, Pons A, Salay TM, McMiller TL, Gilson MM, Wang C, Selby M, Taube JM, Anders R, Chen L, Korman AJ, Pardoll DM, Lowy I, Topalian SL** 2010 Phase I study of single-agent anti-programmed death-1 (MDX-1106) in refractory solid tumors: safety, clinical activity, pharmacodynamics, and immunologic correlates. J Clin Oncol 28:3167–3175

2006 CD45RA on human CD8 T cells is sensitive to the time elapsed since the last antigenic stimulation. Blood 108:2897–2905

THE ENDOCRINE SOCIETY®

Members have FREE online access to the journal *Hormones & Cancer.*

www.endo-society.org/HC